ILL record updated to IN PROCESS
Record 14 of 18

ILL pe Record 14 of 18
CAN YOU SUPPLY ? YES NO COND FUTUREDATE
:ILL: 685481 :Borrower: UBY :ReqDate: 20021011 :NeedBefore: 20021110
:Status: IN PROCESS 20021011 :RecDate: :RenewalReq:
:OCLC: 10180940 :Source: OCLCILL :DueDate: :NewDueDate:
:Lender: *UUM,AFU,AZS,ILU,IXA
:CALLNO: (4) QC 454 M3 I66
:TITLE: International journal of mass spectrometry and ion processes.
:IMPRINT: Amsterdam : Elsevier, c1983-c1998.
:ARTICLE: MCIVER RT: TRAJECTORY CALCULATIONS FOR AXIAL INJECTION OF IONS INTO A MAGNETIC-FIELD - OVERCOMING THE MAGNETIC-MIRROR EFFECT WITH AN RF QUADRUPOLE LENS
:VOL: 98 :NO: 1, June 30TE: :DATE:
:PAGES: 35-50
:VERIFIED: <TN:309656>OCLC ISSN: 0168-1176 [Format: Serial]
:PATRON: Peterson, Bryan

NO CHARGE

ARIEL

:SHIP TO: Brigham Young University ILL
3421 Lee Library
One Lee Lane
Provo, Ut 84602

:BILL TO: same
:SHIP VIA: Library Rate :MAXCOST: 20ifm :COPYRT COMPLIANCE: CCL
:FAX: (801) 422-0471, Phone 801-422-3624
:BILLING NOTES: UMI Account Number #D9522701. ISI ACCT: File #0016890 (**ISI SHIP VIA FEDERAL EXPRESS**)
:BORROWING NOTES: 51-0724 BCR/AMIGOS Code Signer. ARIEL Address: 128.187.229.251 CLient Code ACF17E Please conditional negative replies.
:LENDING CHARGES: :SHIPPED: :SHIP INSURANCE:
:LENDING RESTRICTIONS:
:LENDING NOTES:
:RETURN TO:
:RETURN VIA:

International Journal of Mass Spectrometry and Ion Processes, 98 (1990) 35–50
Elsevier Science Publishers B.V., Amsterdam – Printed in The Netherlands

TRAJECTORY CALCULATIONS FOR AXIAL INJECTION OF IONS INTO A MAGNETIC FIELD: OVERCOMING THE MAGNETIC MIRROR EFFECT WITH AN R.F. QUADRUPOLE LENS

ROBERT T. McIVER, Jr.

Department of Chemistry, University of California, Irvine, CA 92717 (U.S.A.)

(First received 6 October 1989; in final form 5 December 1989)

ABSTRACT

The magnetic mirror effect is one of the problems that must be overcome in order to perform Fourier transform mass spectrometry (FT-MS) experiments with an external ion source. Since the ion source is located outside of the magnetic field, about 1 m from the FT-MS analyzer cell, some type of focusing is needed to guide the ions through the fringing fields of the magnet. Several years ago, McIver and co-workers showed that a quadrupole lens operated in the r.f.-only mode was an effective means for accomplishing this. In this paper, the theory of ion injection by a r.f. quadrupole lens is developed and trajectory calculations are performed to determine how the mass range of the quadrupole lens depends on the frequency and voltage of the signal that is applied to the rods. The calculations show that the quadrupole lens functions like a broadband filter with certain low mass and high mass cut-offs. By selecting the proper operating conditions, the mass range of the injected ions can extend over several thousand mass units and high mass ions (m/z greater than 20000) can be injected.

INTRODUCTION

In Fourier transform mass spectrometry (FT-MS), charged particles are trapped in an analyzer cell by a homogeneous magnetic field, and a mass spectrum is obtained by measuring their cyclotron frequencies [1–4]. Very high mass resolution and high detection sensitivity can be achieved if the pressure in the analyzer cell is below 10^{-8} Torr, but at higher pressures the mass resolution is poor because the coherent cyclotron motion of the ions is interrupted by collisions. For example, under low pressure conditions a peak at m/z 1000 typically has a width of 0.10 u, which corresponds to a mass resolution of 10000, but increasing the pressure to 2×10^{-5} Torr causes the peak to broaden to about 10 u, which corresponds to a resolution of only 100. This is a major limitation that has restricted the applications of FT-MS. Although electron ionization and laser desorption have been used successfully with FT-MS, coupling to a gas or liquid chromatograph or to a fast atom bombardment (FAB) source has proven to be very difficult because these methods greatly increase the pressure in the analyzer cell.

0168-1176/90/$03.50

In 1983, McIver and co-workers proposed that the pressure limitation problems of FT-MS could be overcome by separating the ion production region from the ion detection region [5,6]. To test this idea they built a hybrid instrument called a tandem quadrupole-Fourier transform mass spectrometer [7–9]. Ions formed by electron ionization in a conventional quadrupole mass spectrometer were injected into a FT-MS analyzer cell that was located at the center of a 4.1-T superconducting magnet. The two regions were separately pumped so that elevated pressures in the ion source of the quadrupole mass spectrometer did not spoil the vacuum around the FT-MS analyzer cell. Experiments done in collaboration with Hunt and co-workers demonstrated that the method could provide high resolution mass spectra for low molecular weight peptides ionized by FAB [8,9]. Other advantages were also realized. For example, a variety of ion sources can be attached to the instrument because the ion source is located outside of the magnetic field, about 1 m from the FT-MS analyzer cell. This provides ample room for attaching large vacuum pumps to handle elevated pressures in the ion source. We also found that the peak heights in the mass spectra were more reproducible and the operating conditions of the instrument were more stable, presumably because at low pressures contamination of the electrodes of the FT-MS analyzer cell is greatly reduced.

An important feature of the tandem quadrupole-Fourier transform mass spectrometer is a second quadrupole, denoted Q2, that guides the ion beam from the exit of the quadrupole mass spectrometer to the FT-MS analyzer cell. Without Q2, low energy ions cannot be efficiently injected into the magnetic field because of a phenomenon called the magnetic mirror effect [10]. This problem is overcome by Q2 because it focuses the ions into a narrow beam and enables them to penetrate through the fringing fields of the magnet. In addition, Q2 also functions like a filter so that only ions within a preselected mass range are injected into the analyzer cell. This is an important feature because in FAB experiments the analyzer cell can be easily overloaded to its space charge limit by low mass matrix-related ions.

Steady progress has been made in the development of external ion source FT-MS instruments. Modifications by Hunt et al. to their tandem quadrupole-Fourier transform mass spectrometer have made it possible to record mass spectra on oligopeptides and small proteins in the mass range between 2 and 13 kDa [11,12]. Other investigators have used electrostatic lenses, instead of a r.f. quadrupole lens, to focus the ions and inject them through the fringing magnetic fields [13–17].

Recently we described a new external ion source FT-MS instrument that utilizes a single, long r.f. quadrupole lens to guide ions from the ion source to the analyzer cell [18–20]. A schematic drawing of the new instrument is shown in Fig. 1. The FT-MS analyzer cell is mounted inside a stainless steel tube that

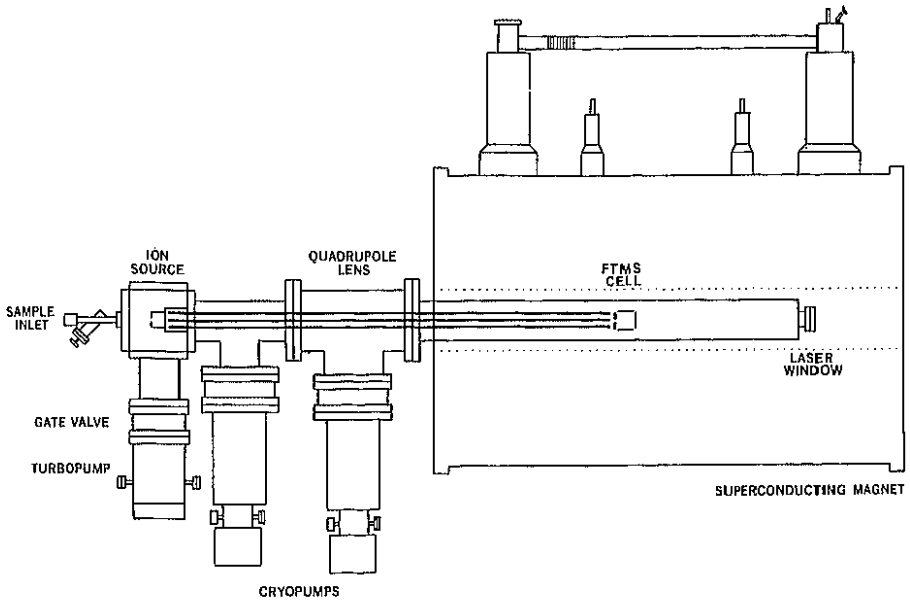

Fig. 1. Schematic drawing of an external ion source Fourier transform mass spectrometer with a r.f. quadrupole lens for focusing the ion beam.

inserts into the bore of a 6-T superconducting magnet. Ions are produced in a source region that is outside the field, 1.2 m away from the analyzer cell. Three large vacuum pumps maintain a pressure gradient as large as 40 000:1 between the ion source and the analyzer cell. This design is simpler and easier to operate than the original tandem quadrupole-Fourier transform mass spectrometer because only two adjustments (the frequency and r.f. voltage of the signal applied to the quadrupole) are needed to control the range of injected ions.

In this paper, a model for the electric and magnetic fields of the new external ion source FT-MS instrument is developed, and trajectory calculations are used to illustrate the effectiveness of a r.f. quadrupole lens for injecting ions axially into a strong magnetic field. The trajectory calculations can also be used to determine how the range of injected masses and the high mass and low mass cut-offs depend on the frequency and voltage of the quadrupole r.f. signal.

THEORY

Model for the magnetic field

Figure 2 shows the axial (B_z) and radial (B_r) components of the magnetic field that were measured by placing a gaussmeter at various distances from the

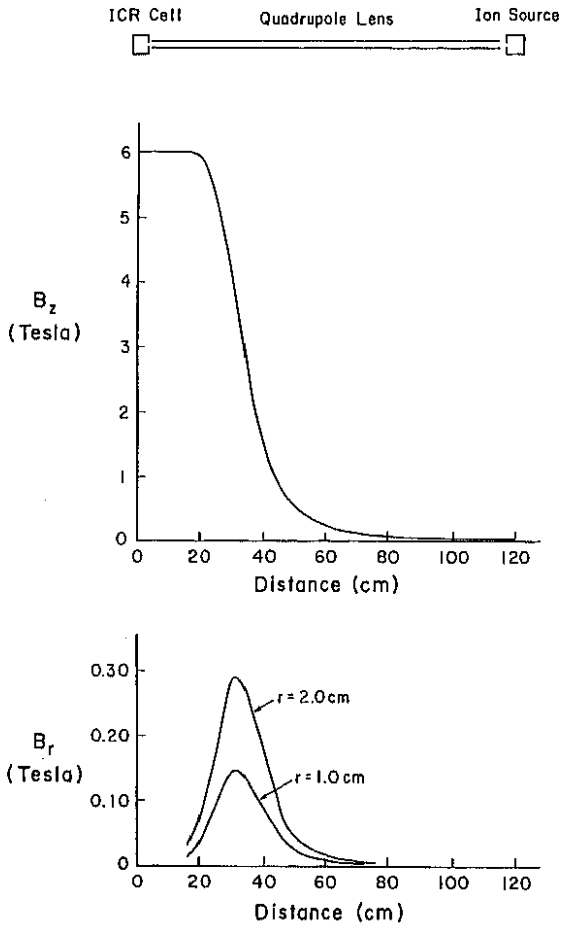

Fig. 2. Magnetic field plots for a 6-T superconducting magnet showing (a) the axial component B_z, and (b) the radial components B_r at various distances from the axis. The relative positions of the FT-MS analyzer cell, quadrupole lens, and ion source are shown at the top of the figure.

center of the magnet. The relative positions of the ion source, quadrupole lens, and analyzer cell are shown at the top of the figure. The field strength at the ion source is 0.02 T, and at the analyzer cell it is 6.0 T. Inside the solenoid the field is very homogeneous, better than one part in 10^5 over a 1 cm^3 volume according to the manufacturer. However, outside of the central region it decreases rapidly and becomes highly inhomogeneous. For example, the radial magnetic field B_r is zero at $r = 0$, but 1 cm off axis it is as large as 0.15 T.

Since the magnetic field is symmetric about the z-axis, the axial and radial components can be related by using Maxwell's equation for a magnetic field [10]

$$\bar{\nabla} \cdot \bar{B} = 0 \tag{1}$$

$$\frac{1}{r}\frac{\partial}{\partial r}(rB_r) + \frac{\partial B_z}{\partial z} = 0 \tag{2}$$

where del is written in circular cylindrical coordinates [9]. Equation 2 can be rearranged and integrated to give

$$B_r = -\frac{1}{r}\int_0^r r'\left(\frac{\partial B_z}{\partial z}\right) \mathrm{d}r' \tag{3}$$

$$B_r = -\frac{r}{2}\left(\frac{\mathrm{d}B_z}{\mathrm{d}z}\right)_{r=0} \tag{4}$$

This result is only valid close to the axis because it assumes, (1) that the rate of change of B_z with respect to z is known at $r = 0$ (as in Fig. 2), and (2) that $\mathrm{d}B_z/\mathrm{d}z$ does not vary much with r. Equation 4 shows that the measured B_z and B_r curves shown in Fig. 2 are related. To test this, Fig. 2 shows that at $z = 30\,\mathrm{cm}$, the slope of B_z is about $-0.29\,\mathrm{T\,cm^{-1}}$. Substituting this value along with $r = 1\,\mathrm{cm}$ into Eq. 4 gives a calculated B_r value of 0.14 T, which is quite close to the measured value.

For the trajectory calculations, the axial magnetic field strength at different positions from the analyzer cell is calculated from analytical fits to the data in Fig. 2(a). This curve is divided into 28 regions, and for each of these the measured B_z values are fitted to an analytical expression of the form

$$B_z = K1 + zK2 + z^2K3 \tag{5}$$

where $K1$, $K2$, and $K3$ are obtained by a linear least-squares fit. The radial component B_r is then calculated from Eq. 4 by taking the derivative of Eq. 5 with respect to z. This gives

$$B_r = (-r/2)(K2 + 2zK3) \tag{6}$$

Since the solenoidal magnetic field is cylindrically symmetric, the components B_x and B_y are calculated as follows.

$$B_x = B_r(x/r) \tag{7}$$

$$B_y = B_r(y/r) \tag{8}$$

Equations of motion

In the presence of an electric field $\bar{E}$ and a magnetic field $\bar{B}$, the equation of motion for a charged particle is

$$m\frac{\mathrm{d}\bar{v}}{\mathrm{d}t} = q\bar{E} + q(\bar{v} \times \bar{B}) \tag{9}$$

where q is the charge of the particle, m is its mass, and v is its velocity. Using

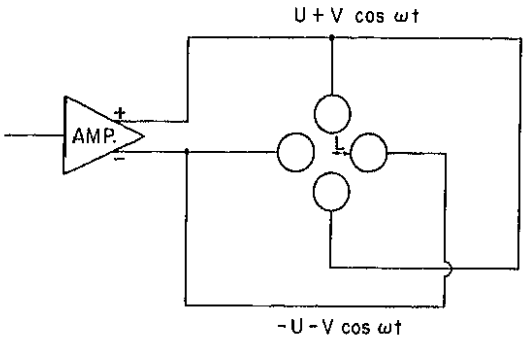

Fig. 3. End view of the quadrupole lens showing the voltages applied to the rods.

a Cartesian coordinate system, the components of the electric and magnetic fields can be written as

$$\bar{E} = E_x\bar{i} + E_y\bar{j} + E_z\bar{k} \tag{10}$$

$$\bar{B} = B_x\bar{i} + B_y\bar{j} + B_z\bar{k} \tag{11}$$

where $\bar{i}$, $\bar{j}$, and $\bar{k}$ are unit vectors. Substitution of these expressions into Eq. 9 followed by evaluation of the cross product terms gives three coupled differential equations for the ion's motion

$$m\frac{dv_x}{dt} = qE_x + q(v_yB_z - v_zB_y) \tag{12}$$

$$m\frac{dv_y}{dt} = qE_y + q(v_zB_x - v_xB_z) \tag{13}$$

$$m\frac{dv_z}{dt} = qE_z + q(v_xB_y - v_yB_x) \tag{14}$$

The electric field term $\bar{E}$ is due to the r.f. and d.c. voltages that are applied to the quadrupole rods. Figure 3 shows an end view of the four rods and the voltage signal $(U + V\cos wt)$ that is applied differentially to opposite pairs of the rods. Under these conditions, the electric potential near the center of the rods is given by

$$\Phi = (U + V\cos wt)\left(\frac{x^2 - y^2}{L^2}\right) \tag{15}$$

where U is the d.c. voltage and V is the base-to-peak r.f. voltage that is applied to the rods, and L is the distance from the center of the assembly to the surface of the rods. In our apparatus, $L = 0.275$ cm, and the diameter of the rods is 0.637 cm. These values were chosen so as to minimize the distortion of the ideal quadrupole potential by the use of round rods [21,22]. The electric field terms needed for the equation of motion are equal to the negative of the

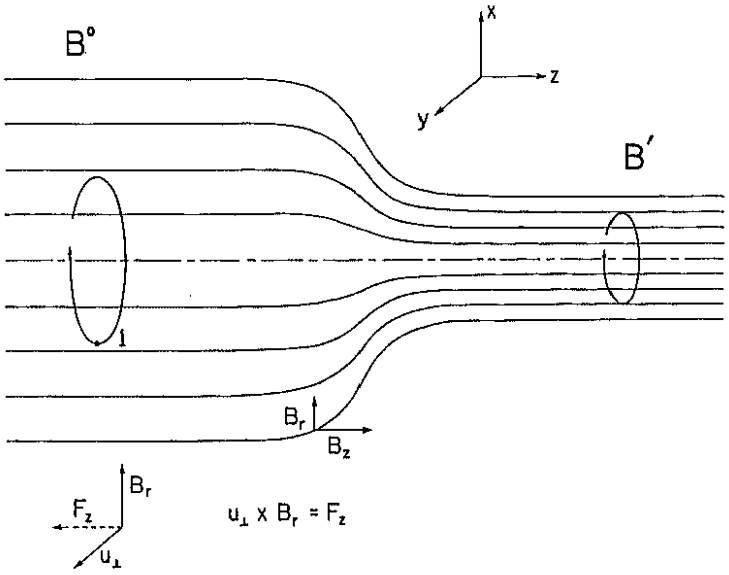

Fig. 4. Illustration of the magnetic mirror effect. As an ion moves from the left to the right (from the low field region to the high field region) it experiences a retarding force F_z.

gradient of the potential. This gives

$$E_x = (U + V\cos wt)\left(\frac{-2x}{L^2}\right) \tag{16}$$

$$E_y = (U + V\cos wt)\left(\frac{2y}{L^2}\right) \tag{17}$$

$$E_z = 0 \tag{18}$$

The trajectory calculations that follow were performed by specifying initial conditions for the position (x, y, z) and velocity (v_x, v_y, v_z) of an ion and then integrating the equations of motion numerically.

RESULTS AND DISCUSSION

Magnetic mirror effect

In order to transfer ions efficiently from an external ion source to a FT-MS analyzer cell, a means must be found to overcome the magnetic mirror effect. This problem is illustrated in Fig. 4. At the far left side of the figure the magnetic field lines of force are pointed primarily in the z direction and the radial component B_r is zero. At the center of the figure, however, B_r becomes quite significant as the field lines converge. The large circle at the left represents the cyclotron orbit of a positive ion, centered about $r = 0$. At

position 1 the ion has a perpendicular component of velocity $u_\perp$. The coordinate diagram at the lower part of Fig. 4 shows that the cross product of $u_\perp$ and B_r gives a force F_z that opposes the motion of the ions as they move from the low field region into the high field region. The magnitude of this force is

$$F_z = qu_\perp B_r \tag{19}$$

where q is the charge of the ion. Substituting Eq. 4 for B_r gives

$$F_z = -\tfrac{1}{2}qu_\perp r\left(\frac{dB_z}{dz}\right) \tag{20}$$

where r is now the radius of gyration for the ion's cyclotron orbit. This equation shows the origin of the magnetic mirror effect. Because F_z is directed opposite to the forward motion of the ion, the ion encounters stiff resistance as it attempts to move into the region of high field strength.

Another important aspect of the magnetic mirror effect can be derived by applying the law of conservation of angular momentum to the situation depicted in Fig. 4. The angular momentum associated with the ion's cyclotron motion is given by $mu_\perp r$, the product of its mass, radial velocity, and radius of gyration. Combining this with the formulas for the ion's radius of gyration ($r = u_\perp/w$) and cyclotron frequency ($w = qB/m$) gives $(mu_\perp)^2/qB$ for the angular momentum. Since the angular momentum must remain constant as the particle moves from the low field region B^0 to the high field region B', we can write

$$\frac{(mu_\perp^0)^2}{qB^0} = \frac{(mu'_\perp)^2}{qB'} \tag{21}$$

where $u_\perp^0$ and $u'_\perp$ are the ion's radial velocity components in the low field and high field regions, respectively. Cancelling the m and q terms in Eq. 21 gives the fundamental equation for the magnetic mirror effect:

$$\left(\frac{u_\perp^0}{u'_\perp}\right)^2 = \frac{B^0}{B'} \tag{22}$$

Another form of this expression can be derived by rearranging Eq. 22 and substituting the radial translation energy, $E_\perp = mu^2/2$, in place of u^2. This gives

$$E'_\perp = E_\perp^0\left(\frac{B'}{B^0}\right) \tag{23}$$

Equation 23 specifies that the ion's radial translation energy must increase as it moves from a region of low field strength B^0 to a region of high field strength B'.

These concepts are illustrated in Fig. 5 by three trajectories which show the

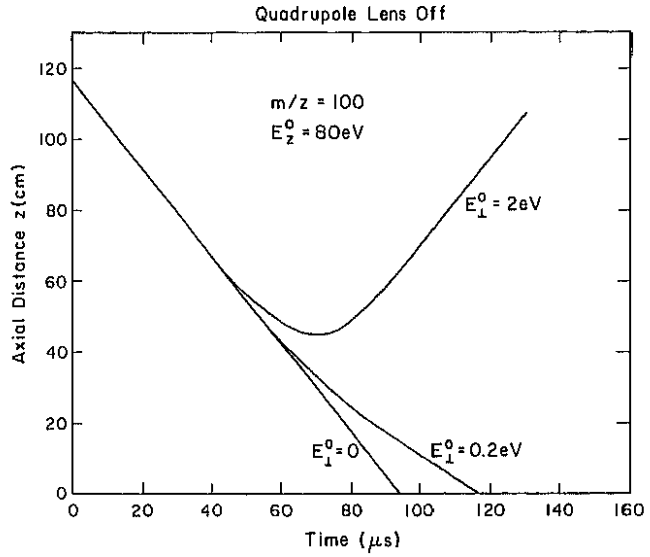

Fig. 5. Calculated trajectories for m/z 100 ions injected axially into a 6-T superconducting magnet without any focusing by the quadrupole lens. Initial conditions: quadrupole r.f. and d.c. voltages zero, $x^0 = y^0 = 0$, $z^0 = 117$ cm, axial energy $E_z = 80$ eV.

axial distance (z) of an ion from the FT-MS analyzer cell as a function of time. The trajectories are calculated by solving Eqs. 12–14 with the electric field terms set to zero. In each case the assumed initial conditions are the same (m/z 100, $x^0 = y^0 = 0$, $z^0 = 117$ cm, and axial energy 80 eV). Only the initial radial energies are different. For the first case, $E_\perp^0 = 0$, the ion moves in a straight line directly down the bore of the magnet and reaches the FT-MS analyzer cell after a flight time of 94 μs. There is no deflection by the magnetic field, and the final axial energy is the same as its initial value, just as expected from Eq. 23. The second trajectory, which assumes $E_\perp^0 = 2$ eV, is an example of the magnetic mirror effect. The ion slows down as it moves into a magnetic field, and when it is 44 cm from the analyzer cell its forward motion ceases ($dz/dt = 0$) and it is reflected back toward the ion source. According to the trajectory calculation, the turn around point occurs when the magnetic field strength is 0.877 T. This is very close to the value 0.88 T that one would calculate from Eq. 23 by substituting $E_\perp^0 = 2.0$ eV and $B^0 = 0.022$ T at the ion source and $E'_\perp = 80$ eV at the reflection point (where all the initial axial energy is converted into radial energy). For the third case, $E_\perp^0 = 0.2$ eV, the ion is decelerated slightly by the magnetic field, but it is still able to reach the analyzer cell. The results for this trajectory are replotted in Fig. 6 to illustrate how the axial and radial energies change as an ion moves toward the analyzer cell. The ion source, quadrupole lens, and FT-MS analyzer cell are shown at the top of the figure, but for this example the quadrupole is turned off. Figure

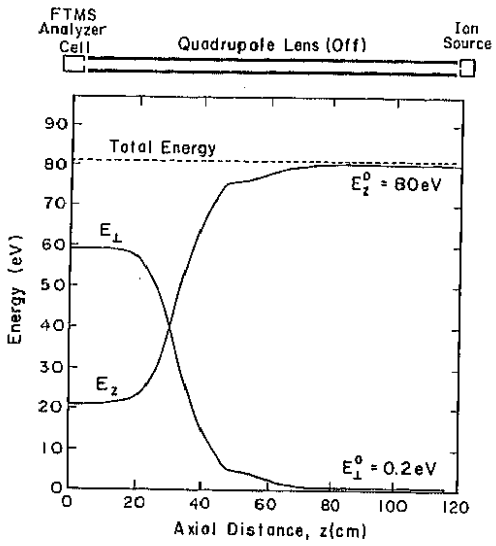

Fig. 6. Variation of axial and radial energy as an ion moves from the ion source to the FT-MS analyzer cell with no voltages applied to the quadrupole lens. The initial conditions for the trajectory were the same as those of Fig. 5.

6 shows that although the total energy remains constant during the trajectory, the axial energy decreases from 80 eV to 21.1 eV and the radial energy increases from 0.2 eV to 59.2 eV as the ion moves from the ion source to the analyzer cell. Although this trajectory looks very similar to the case for $E_\perp^0 = 0$, there is a big difference because so much of the axial energy is converted to radial energy. This agrees closely with what would have been predicted simply from Eq. 23. For example, substituting $E_\perp^0 = 0.2$ eV and $B^0 = 0.022$ T for the initial conditions and $B' = 6.05$ T for the magnetic field strength at the analyzer cell gives 55 eV for the calculated radial energy of the injected ion. The two values are not exactly the same because the trajectory calculation assumes an initial starting point on the axis ($x^0 = y^0 = 0$), whereas Eq. 23 assumes that the cyclotron orbit is centered about the axis.

Figure 7 shows three trajectories for m/z 15 000 ions having different initial radial energies but the same axial energy (80 eV) and initial conditions as in Fig. 5. As before, ions with zero radial energy move straight down the axis of the magnet and suffer no deceleration. The flight time is considerably longer (1153 μs vs. 94 μs for m/z 100), but otherwise the trajectory is the same even for such a high mass ion. The other two trajectories in Fig. 7 show that reflection of m/z 15 000 ions by the magnetic field is very similar to that for the low mass ions. This is expected, of course, because according to Eq. 23 the trajectory is determined primarily by the radial energies and magnetic fields.

These trajectory calculations and the simple equations for the magnetic

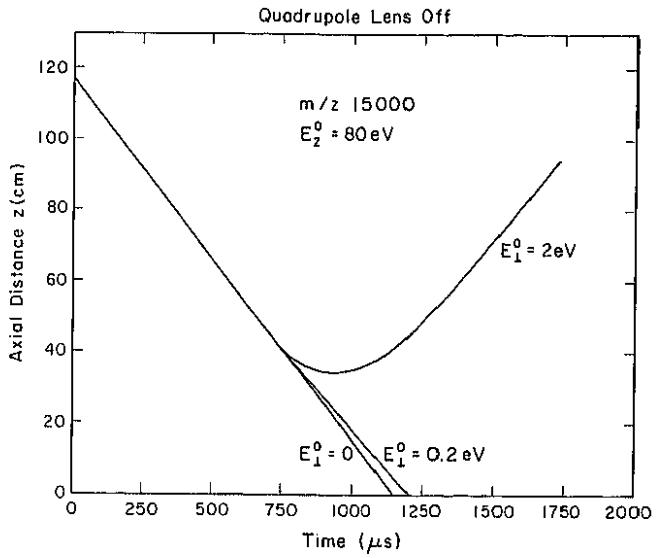

Fig. 7. Calculated trajectories for m/z 15 000 injected axially into a 6-T superconducting magnet without any focusing by the quadrupole lens. Initial conditions: quadrupole r.f. and d.c. voltages zero, $x^0 = y^0 = 0$, $z^0 = 117$ cm, axial energy $E_z = 80$ eV.

mirror effect show that it is difficult to inject ions into a magnetic field and that those that are injected successfully have a wide distribution of axial and radial energies. The key to overcoming these problems is revealed by Eq. 20: the radial velocity $u_\perp$ must be minimized, and the ion beam must be well focused so that it passes directly down the center of the solenoid. If these conditions are met, the decelerating force F_z is minimized and ions with low axial energies can be injected. The trajectory calculations in the next section demonstrate that a r.f. quadrupole lens is very effective at focusing and injecting the ions.

Focusing by a r.f. quadrupole lens

In order to overcome the magnetic mirror effect, we utilize a r.f. quadrupole lens to focus the ion beam and direct it straight down the bore of the superconducting solenoidal magnet. This is illustrated in Table 1 by a side-by-side comparison of the calculated trajectory for m/z 1000 with and without the quadrupole lens. The initial conditions are the same as in Figs. 5–7. The first two columns of Table 1 show the flight time and distance of the ion from the FT-MS analyzer cell, as in Fig. 5. When the quadrupole lens is turned off (U and $V = 0$), the ion is reflected by the magnetic field. The deceleration caused by the magnetic mirror effect is evidenced by the sharp decrease in E_z and increase in $E_\perp$ after about 178 μs. Reflection occurs when the ion is 42 cm from

TABLE I

Effect of a quadrupole lens on the trajectory of an m/z 1000 ion injected into a 6-T magnet

Time (μs)	Quadrupole off ($V = 0$)			Quadrupole on ($V = 100$ V)		
	z (cm)	$E_\perp$ (eV)	E_z (eV)	z (cm)	$E_\perp$ (eV)	E_z (eV)
0.0	117.0	2.0	80.0	117.0	2.0	80.0
19.8	109.2	2.0	80.0	109.2	2.0	80.0
39.6	101.4	2.0	80.0	101.4	1.4	80.0
59.4	93.7	2.0	80.0	93.7	0.9	80.0
79.2	85.9	2.1	79.9	85.9	1.9	80.0
99.0	78.1	2.2	79.8	78.1	1.7	80.0
118.8	70.4	2.7	79.3	70.3	1.1	80.0
138.6	62.7	4.6	77.4	62.5	0.2	80.0
158.4	55.2	12.7	69.3	54.8	1.8	80.0
178.2	48.5	37.6	44.6	47.0	2.9	80.0
198.0	44.2	72.5	9.5	39.2	1.6	80.0
217.8	42.4	79.4	2.6	31.4	1.5	79.7
237.6	42.2	77.1	4.9	23.7	4.8	79.2
257.4	46.5	35.4	46.6	16.0	3.7	79.1
277.2	52.9	26.2	55.8	8.2	2.2	79.1
297.0	59.4	24.8	57.2	0.0	3.6	79.1
316.8	66.0	23.2	58.8			
336.1	72.8	21.7	60.3			
356.4	79.6	20.3	61.7			
376.2	86.4	19.2	62.8			
396.0	93.4	18.3	63.7			
415.8	100.3	17.6	64.6			

the analyzer cell, and afterward the z values increase as the ion moves away. For comparison, the sixth and seventh columns show how the radial and axial energies change when the quadrupole lens is driven by a 100 V, 1.0 MHz signal. Under these conditions, the ion is successfully injected after a flight time of 297 μs and the axial and radial energies are only slightly different from their initial values. This is generally what is found from the trajectory calculations. The r.f. quadrupole lens focuses the ions into a tight beam of less than a millimeter diameter and guides them through the fringing fields of the magnet. According to Eq. 20, this method is successful because F_z, the decelerating force which causes the magnetic mirror effect, is equal to zero when the ions are injected exactly down the center of the solenoid ($r = 0$).

The effectiveness of the quadrupole lens can be understood by comparing the magnitudes of the electric and magnetic forces on an injected ion. The force of the quadrupole lens is given by

$$\text{Quadrupole force} = 2qxV/L^2 \tag{24}$$

where q is the charge of the ion, x is its displacement from the center of the quadrupole lens, V is the r.f. voltage on the rods, and L is the separation of the rods. This force pushes the ions back toward the center of the quadrupole rod assembly. Substituting typical values ($q = 1.602 \times 10^{-19}$ C, $x = 1 \times 10^{-4}$ m, $V = 400$ V, $L = 2.75 \times 10^{-3}$ m) gives 1.69×10^{-15} N.

For comparison, the force of the magnetic field is

$$\text{Magnetic field force} = qvB \tag{25}$$

where v is the velocity of the ion and B is the magnetic field strength. Substituting typical values ($q = 1.602 \times 10^{-19}$ C, $v = 2 \times 10^{4}$ m s^{-1} and $B = 6$ T) gives 1.92×10^{-19} N, which is several orders of magnitude smaller than the electric force. As a result, the trajectory of an ion is determined primarily by the quadrupole lens, and when the proper operating parameters are chosen the quadrupole lens can overcome the magnetic mirror effect.

Range of masses injected

Another feature of the quadrupole lens is that it can be used to select which ions are transported to the analyzer cell. Basically, it functions like a bandpass filter with an adjustable high mass and low mass cut-off. The low mass cut-off is important for experiments with a FAB source because the dynamic range of the analyzer cell is limited and it can be easily filled to its space charge limit by uninteresting matrix-related ions.

The filtering performance of a quadrupole lens is illustrated by the three graphs in Fig. 8. Figure 8a shows that when the quadrupole is driven with a 200 V, 1 MHz signal all ions between m/z 475 and 2200 are injected. The low mass cut-off, m/z 475, is very sharp and is independent of the initial conditions. However, the high mass cut-off is very dependent on the initial radial energy of the ions. For example, m/z 2200 is the high mass cut-off for ions having a radial energy of 5 eV, but for ions having a radial energy of 1 eV the high mass cut-off extends out to about m/z 13 000. Figure 8b shows that increasing the quadrupole voltage to 400 V extends the high mass limit to m/z 9800, even for ions with 5 eV of radial energy. This confirms our earlier observations that high r.f. voltages are needed to transmit high mass ions [18,20]. The calculations also show that the low mass limit is raised to m/z 750, and generally both the high mass and low mass limits increase as the quadrupole r.f. voltage is increased. In order to inject low mass ions with our present apparatus, it is necessary to operate the quadrupole at either a lower voltage and/or a higher frequency. For example, Fig. 8c shows that 200 V and 3 MHz transmits ions in the range m/z 90 to m/z 650. As before, the high mass limit depends primarily on the initial radial energy of the ions with low energy ions being easier to inject.

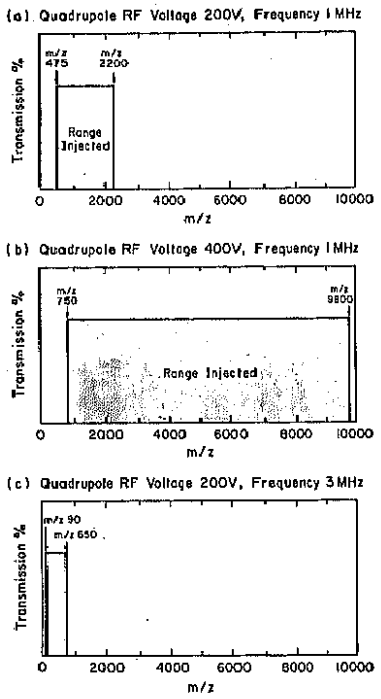

Fig. 8. The bandpass of the r.f. quadrupole lens depends on the frequency and voltage of the applied signal: (a) r.f. -only mode: 200 V, 1 MHz, (b) r.f.-only mode: 400 V, 1 MHz, (c) r.f.-only mode: 200 V, 3 MHz.

One of the conclusions from this study is that the initial radial energy of the ions is a very important factor in determining whether they are injected successfully. This is especially important for high mass ions. Figure 9 shows the minimum r.f. voltage that is needed to successfully inject m/z 1000 and m/z 10 000 ions having different initial radial energies. It is assumed that the operating frequency of the quadrupole is 1 MHz and the initial axial energy is 80 eV. This figure shows that zero r.f. voltage is needed if the radial energy of the ions is zero. Although ions having 2 eV of radial energy would normally be reflected by the magnetic mirror effect, an r.f. voltage of 85 V is sufficient to inject m/z 1000 ions and 260 V is sufficient to inject m/z 10 000 ions. Generally, the r.f. voltage has to be increased to confine and focus ions having higher radial energies.

In conclusion, trajectory calculations have shown that a r.f. quadrupole lens is an effective means for focusing an ion beam and enabling it to be injected into a magnetic field. Conventional quadrupole mass spectrometers are usually thought of as having a limited mass range and low transmission efficiency, but this results because of the d.c. voltages that are used to narrow the transmission bandwidth. The r.f.-only operating mode has very different

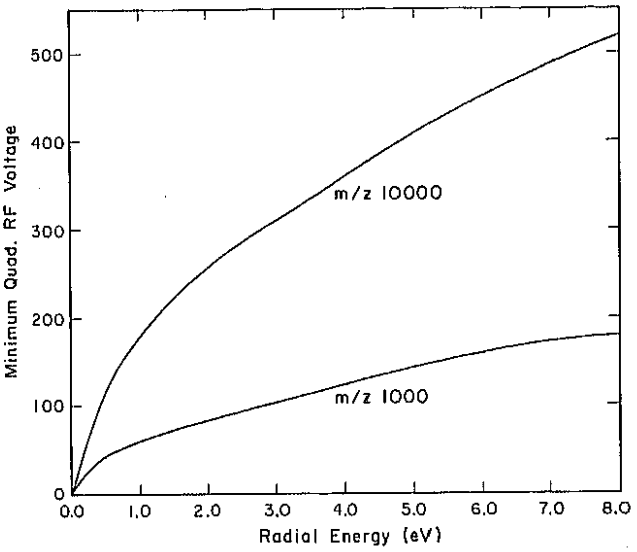

Fig. 9. Calculated minimum quadrupole r.f. voltage that is needed to inject ions having various initial radial energies. Assumed initial conditions are the same as those of Fig. 5 and the quadrupole frequency is 1 MHz.

characteristics: a broad range of masses between certain high mass and low mass cut-offs are transmitted. Under these conditions the injection efficiency is very high and the upper mass limit can extend at least up to m/z 30 000.

REFERENCES

1 M.L. Gross and D.L. Rempel, Science, 226 (1984) 261.
2 D.A. Laude, Jr., C.L. Johlman, R.S. Brown, D.A. Weil and C. Wilkins, Mass Spectrom. Rev., 5 (1986) 107.
3 A.G. Marshall, Acc. Chem. Res., 18 (1985) 316.
4 D.H. Russell, Mass Spectrom. Rev., 5 (1986) 167.
5 R.T. McIver, Jr., R.L. Hunter, M.S. Story, J. Syka and M. Labunsky, paper presented at the 31st Annual Conference on Mass Spectrometry and Allied Topics; Boston, MA, 8–13 May 1983.
6 R.T. McIver, Jr., U.S. Patent 4,535,235, Apparatus and Method for Injection of Ions into an Ion Cyclotron Resonance Cell, Aug. 13, 1985.
7 R.T. McIver, Jr., R.L. Hunter and W.D. Bowers, Int. J. Mass Spectrom. Ion Processes, 64 (1985) 67.
8 D.F. Hunt, J. Shabanowitz, R.T. McIver, Jr., R.L. Hunter and J.E.P. Syka, Anal. Chem., 57 (1985) 765.
9 D.F. Hunt, J. Shabanowitz, J.R. Yates III, R.T. McIver, Jr., R.L. Hunter, J.E.P. Syka and J. Amy, Anal. Chem., 57 (1985) 2728.
10 F.F. Chen, Introduction to Plasma Physics, Plenum Press, 1974, p. 29.
11 D.F. Hunt, J. Shabanowitz, J.R. Yates, Jr., N.-Z. Zhu, D.H. Russell and M.E. Castro, Proc. Natl. Acad. Sci. U.S.A., 84 (1987) 620.
12 D.F. Hunt, J. Shabanowitz and J.R. Yates, Jr., J. Chem. Soc., Chem. Commun., (1987) 548.

13 P. Kofel, M. Allemann, Hp. Kellerhals and K.P. Wanczek, Int. J. Mass Spectrom. Ion Processes, 65 (1985) 97.
14 P. Kofel, M. Allemann, Hp. Kellerhals and K.P. Wanczek, Int. J. Mass Spectrom. Ion Processes, 72 (1986) 53.
15 J.M. Alford, P.E. Williams, D.J. Trevor and R.E. Smalley, Int. J. Mass Spectrom. Ion Processes, 72 (1986) 33.
16 J.M. Alford, F.D. Weiss, R.T. Laaksonen and R.E. Smalley, J. Phys. Chem., 90 (1986) 4480.
17 R.E. Smalley, Anal. Instrum., 17 (1988) 1.
18 C.B. Lebrilla, I.J. Amster and R.T. McIver, Jr., Int. J. Mass Spectrom. Ion Processes, 87 (1989) R7.
19 C.B. Lebrilla, D.T.-S. Wang, T.J. Mizaguchi and R.T. McIver, Jr., J. Am. Chem. Soc., 111 (1989) 8593.
20 C.B. Lebrilla, D.T.-S. Wang, R.L. Hunter and R.T. McIver, Jr., Anal. Chem., in press.
21 I.E. Dayton, F.C. Shoemaker and R.F. Mozley, Rev. Sci. Instrum., 25 (1954) 485.
22 D.R. Denison, J. Vac. Sci. Technol., 8 (1971) 266.